Quantum Chemical Study of Hydroxychloroquine and Chloroquine Drugs Used as a Treatment of COVID-19

Chafai, Nadjib**+; Benbouguerra, Khalissa; Chafaa, Salah; Hellal, Abdelkader

Laboratory of Electrochemistry of Molecular Materials and Complex (LEMMC), Department of Process Engineering, Faculty of Technology, University of Ferhat ABBAS Setif-1, El-Mabouda Campus, 19000 Sétif, ALGERIA

ABSTRACT: *Two drugs have been authorized by the Algerian health Ministry to be used in Algeria to treat coronavirus disease 2019 (COVID-19) patients, once is Hydroxychloroquine (HCQ) and the other is Chloroquine (CQ). These drugs have been theoretically studied in order to know their active sites, and vibrational and electronic properties using Density Functional Theory (DFT) at the B3LYP/6-31G (d.p) level. The optimized molecular structures, the vibrational spectra, the HOMO and LUMO properties, dipole moments, Molecular Electrostatic Potentials (MEP), and atomic charges are calculated. In addition, the reactivity of drug molecules has been discussed by calculating some descriptors such as energy gap, hardness, local softness, electronegativity, and electrophilicity.*

KEYWORDS: *Coronavirus; COVID-19; Pandemic; Hydroxychloroquine; Chloroquine; DFT.*

INTRODUCTION

Coronavirus disease 2019 (**COVID-19**) appeared for the first time in Wuhan city, China in December 2019, then it began to spread rapidly in Chinese territory and outside [1, 2]. After about two and a half months of its appearance, the epidemic of COVID-19 was declared a pandemic by the WHO [3]. Generally, the COVID-2019 virus causes diseases in the upper respiratory tract and gastrointestinal, especially in immune-compromised individuals [4].

Currently, there is no known special, efficient, confirmed, pharmacological treatment against COVID-19. However, there are several experiments have been effected on old antimalarial drugs in order to study their effectiveness in the treatment of COVID-19 patients. In this context, Hydroxychloroquine (HCQ) and Chloroquine (CQ) drugs (Fig.1) have been considered a target in most studies. Fig.1 indicates that the molecular structures of CQ and HCQ contain nitrogen and chlorine. Generally, the N and Cl atoms have an important role in biological processes. Chlorinated and nitrogen organic derivatives are considered promising compounds used in medicinal chemistry [5]. Also, the presence of nitrogen and chlorine atoms played an essential role in several biologically active molecules such as the antibiotics Chloramphenicol [6], Clindamycin [7], Griseofulvin, and Vancomycin [8].

A recent article announced that the treatment containing Chloroquine and Remdesivir drugs presents an inhibitive effect on the growth and development processes of SARS-CoV-2 *in vitro* [9]. Also, a clinical test performed on COVID-19 Chinese patients illustrated that Chloroquine had an important effect on the clinical results and viral clearance [10, 11]. In March 2020, parameters [15-17].

** To whom correspondence should be addressed.*
+ E-mail: : n.chafai@univ-setif.dz & nadjib82@gmail.com
1021-9986/2022/1/27-36 10/$/6.00

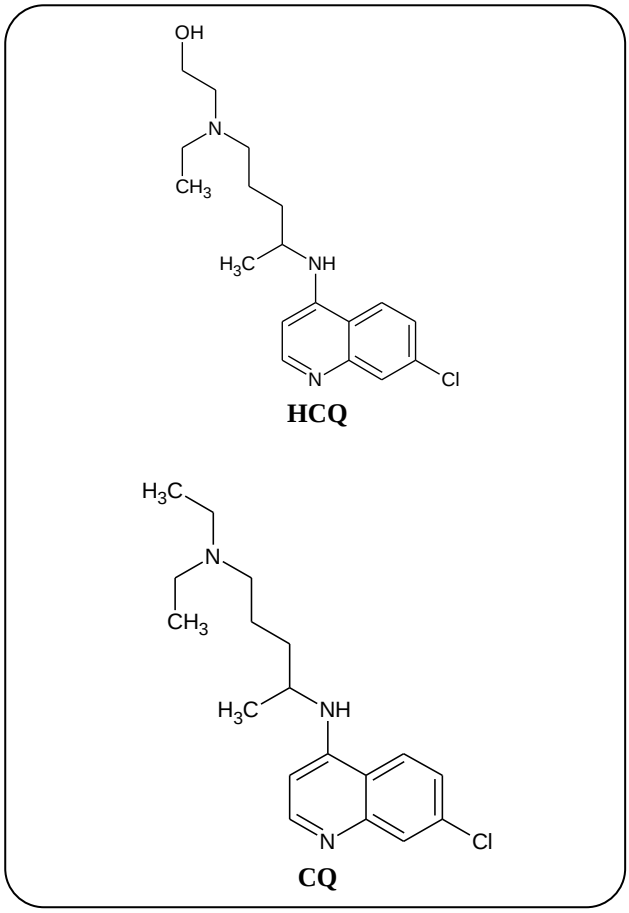

Fig. 1: Chemical structures of Hydroxychloroquine (HCQ) and Chloroquine (CQ).

Didier Raoult et al tested the effect of Hydroxychloroquine In COVID-19 patients, the obtained results indicate that this treatment is extensively related to viral load reduction/disappearance in COVID-19 patients and its effect is reinforced by Azithromycin [12].

Generally, the modes of action of Hydroxychloroquine and Chloroquine are still not completely explicated. Numerous studies revealed that both drugs interfere with the glycosylation of ACE2 receptors, blocking virus/cell fusion and inhibiting lysosomal activity and autophagy by increasing endosomal pH [13] In addition, the clinical effectiveness and side-effect profiles of these drugs can be explained by their mechanisms of action [14].

Generally, the activity of drug molecules is related to their physicochemical and electronic characteristics. Also, the quantum chemical calculations using Density Functional Theory (DFT) method can be used effectively to determine the active sites of drug molecules and to correlate their activity with some quantum chemical In this context, the DFT calculations are extensively used to study the various biological activities of the bioactive molecules [18-20, 21].

The work presented in this paper contains new results of a quantum chemical study of Hydroxychloroquine (HCQ) and Chloroquine (CQ). The reason to select the HCQ and CQ is due to the official adoption of these drugs to treat COVID-19 patients in our country (Algeria), where they have revel a remarkable improvement in the clinical status of patients. So, these two drugs have been theoretically studied to determine their active sites, and vibrational and electronic properties using DFT method at the B3LYP/6-31G (d.p) level. The optimized molecular structures, the vibrational spectra, the Highest Occupied Molecular Orbital (HOMO) and Lowest Unoccupied Molecular Orbital (LUMO) properties, dipole moments (μ), Molecular Electrostatic Potentials (MEP) maps, atomic charges, HOMO-LUMO energy gap (ΔE_{GAP}), hardness (η), local softness (σ), electronegativity (χ) and electrophilicity (ω) are calculated for of the studied drugs.

Computational details

During this study, we utilized the Gaussian 09W program package to carry out all quantum chemical calculations [22]. The geometries of HCQ and CQ were completely optimized by applying the DFT method through B3LYP hybrid functional at 6-31G (d,p) basis set [23, 24]. Also, the same level of theory has been used to calculate the vibrational frequencies at the optimal structures of HCQ and CQ. Additionally, the obtained values of the highest occupied molecular orbital energy (E_{HOMO}) and lowest unoccupied molecular orbital energy (E_{LUMO}) have been used to calculate some quantum chemical parameters such as the energy gap (ΔE_{GAP}), dipole moments (μ), hardness (η), local softness (σ), electronegativity (χ) and electrophilicity (ω). Also, the equations listed below were used to calculate the precedent parameters [25, 26]:

$$\Delta E_{GAP} = E_{LUMO} - E_{HOMO} \quad (1)$$

$$\eta = \frac{E_{LUMO} - E_{HOMO}}{2} \quad (2)$$

$$\sigma = \frac{1}{\eta} \quad (3)$$

$$\chi = \frac{-\left(E_{LUMO} + E_{HOMO}\right)}{2} \quad (4)$$

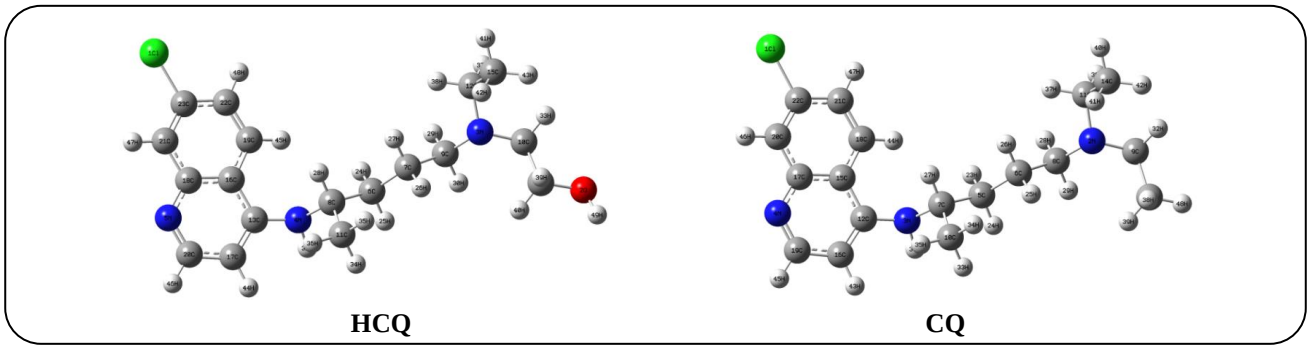

Fig. 2: Optimized structures of Hydroxychloroquine (HCQ) and Chloroquine (CQ).

$$\omega = \frac{\chi^2}{2\eta} \quad (5)$$

RESULTS AND DISCUSSION

Optimized molecular structures

The calculated optimized geometries of HCQ and CQ molecules are presented in Fig.2. In addition, the obtained values of total energy at these optimal structures were -37743.4676 eV for HCQ and -35718.1028eV for CQ, indicating that HCQ is more stable than CQ. From Fig.2, we can see clearly that the addition of the hydroxyl functional group (OH) causes a few modifications in the geometric parameters of HCQ.

Vibrational analysis

The calculated IR spectra of the investigated drugs using DFT method at B3LYP/6-31G (d.p) basis set are presented in Fig. 3. Also, the obtained values of wavenumber for the selected vibrations are summarized in Table 1. The interpretation of these spectra shows the presence of the following selected vibrations:

O-H vibrations

The hydroxyl functional group is considered one of the most dominant and characteristic of all of the infrared group frequencies. Generally, the O-H bond peak is intense because it has a large dipole moment. The characteristic OH functional group of HCQ appeared at 3877 cm^{-1} as a low-intensity peak, which is attributed to the O-H stretching vibration. Also, the medium peak situated at 1121.72 cm^{-1} is due to the C-OH stretching vibration. The broad peak that appeared at 668 cm^{-1} is assigned to the *out-of-plane* O-H bend, or O-H wag. Moreover, the O-H *in-plane* bend vibration appears at 1335 cm^{-1}, which involves the hydrogen bending up and down in the plane of the HCQ molecule.

N-H stretching vibrations

Generally, the N-H stretching vibrations are easily identified by the apparition of a sharp peak at the highest wavenumbers. For the studied drugs, the stretching frequencies of N-H of the secondary amine attached to the aromatic ring were observed at 3716.48 cm^{-1} for HCQ and 3716.46 cm^{-1} for CQ. Moreover, the N-H *out-of-plane* bending vibrations are located 737.55 cm^{-1} for HCQ and 737.98 cm^{-1} for CQ. Also, the weak N-H bending vibrations of the studied drugs are visible at 1500 to 1600 cm^{-1}.

C-H vibrations

Generally, the attributions of CH_2 group frequency include six fundamental modes namely, CH_2 symmetric stretch, asymmetric stretch, rocking, and scissoring which belong to *in-plane* vibration and *out of plane* vibration namely CH_2 twisting and wagging vibration modes. Usually, the region situated between 1500 and 800 cm^{-1} is attributed to the CH_2 wagging, scissoring, rocking, and twisting. For both drug molecules, the observed peaks between 3425 and 3358 cm^{-1} can be attributed to the aromatic C-H stretching vibrations. Also, the aliphatic C-H stretching vibrations appeared between 3288.98 and 3131.86 cm^{-1} for HCQ and 3284.96 and 3126.77 cm^{-1} for CQ. On the other hand, the C-H *out of plane* bending vibrations are situated between 1038.78 and 809.97 cm^{-1} for HCQ and between 1028.6 and 805.63 cm^{-1} for CQ, whereas the C-H *in-plane* bending vibrations are obtained at 1231 cm^{-1} for both molecules.

Aromatic Vibrations

The characteristic peaks of the C-C aromatic stretching vibrations for the HCQ and CQ molecules are observed between 1794 cm^{-1} and 1733 cm^{-1}. Generally, the substitution of the aromatic rings by the chlorine and nitrogen groups affects the majority of the ring vibrational modes.

Table 1: Calculated values of wavenumber for the selected vibrations of HCQ and CQ.

Assignement	Vibrational frequency (cm^{-1})	
	HCQ	CQ
ν(O □ H)	3877.76	-
ν(N □ H)	3716.48	3716.46
$\nu(C \square H)_{Ar}$	3425.33-3358.37	3425.31-3358.34
$\nu(C \square H)_{Alph}$	3288.98-3131.86	3284.96-3126.77
$\nu(C \square C)_{Ar}$	1794.11-1733.40	1794.08-1733.38
ν(C □ N)	1219.70	1218.88
ν(C □ Cl)	674.72	674.36
δ(C □ H)	1038.78-809.97	1028.6-805.63
δ(N □ H)	737.55	737.98

ν: stretching, δ : out of plane bending

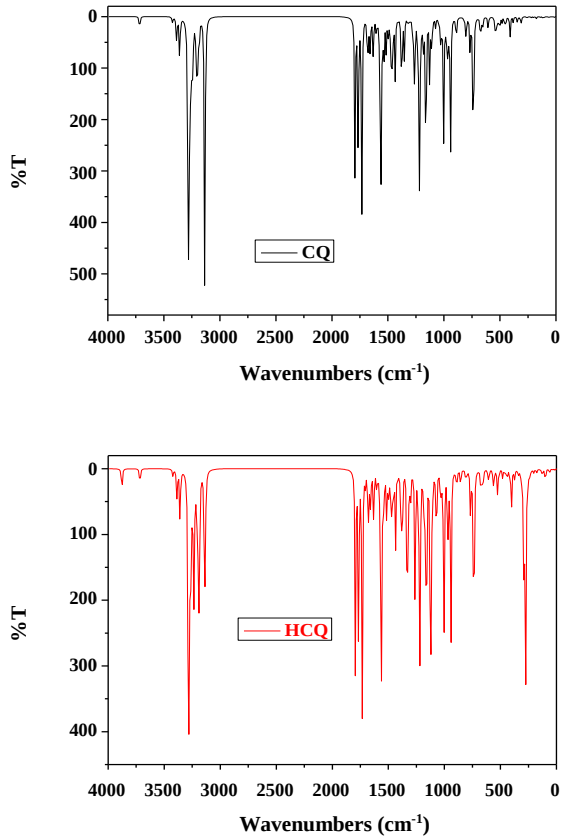

Fig. 3: Calculated IR spectra of HCQ and CQ.

C-N and C=N vibrations

The characteristic peaks of the C-N stretching vibrations of the secondary aromatic amine are observed at 1219.70 cm^{-1} for HCQ and 1218.88 cm^{-1} for CQ. The characteristic peaks of the C=N aromatic stretching vibrations for both drags have appeared at 1732cm^{-1}.

C-Cl vibrations

In general, the analysis of the spectra of compounds involving one or more halogens would appear to be easy. So, the functionality is simple for one single halogen atom connected to carbon. According to the polar nature of the halogen groups, it can be expected the spectral contribution to be characteristic. The characteristic frequencies of C-Cl stretching vibrations of the studied drugs are situated at 674.72 cm^{-1} for HCQ and 674.36 cm^{-1} for CQ.

Frontier molecular orbital analysis

In quantum chemistry, the HOMO and LUMO orbitals and their energies are considered very helpful and very significant parameters to describe the reactivity and stability of the molecule. Generally, the examination of the HOMO gives an idea about the ability of a molecule to donate electrons to an electrophilic species of lower energy MO, whereas the examination of the LUMO characterizes the affinity of a molecule to receive electrons from nucleophilic species [27]. The examination of the HOMO shows the regions of the drug molecule that can contribute electrons to an electrophilic species. As a result, the elevated values of E_{HOMO} are favorable to indicate the capability of a molecule to contribute electrons to an acceptor molecule [28], while the power of a molecule to accept electrons is favored by the low values of E_{LUMO} [29]. Further, the E_{LUMO} indicates the capability of a molecule to take electrons using π* orbitals to form π-back bonds [28]. Moreover, the determination of the energy gap (ΔE_{GAP}) of a molecule is very useful to measure its stability and reactivity [30]. Also, the charge transfer interactions inside the molecule can be explained by the values of ΔE_{GAP}. On the other hand, the energy difference between HOMO and LUMO orbitals measures the necessary energy to excite a molecule. So, when this energy is smaller the molecule can be excited easily, become unstable, and presents a high chemical reactivity. Contrariwise, if ΔE_{GAP} is very large the molecule will present high stability and low chemical reactivity [31].

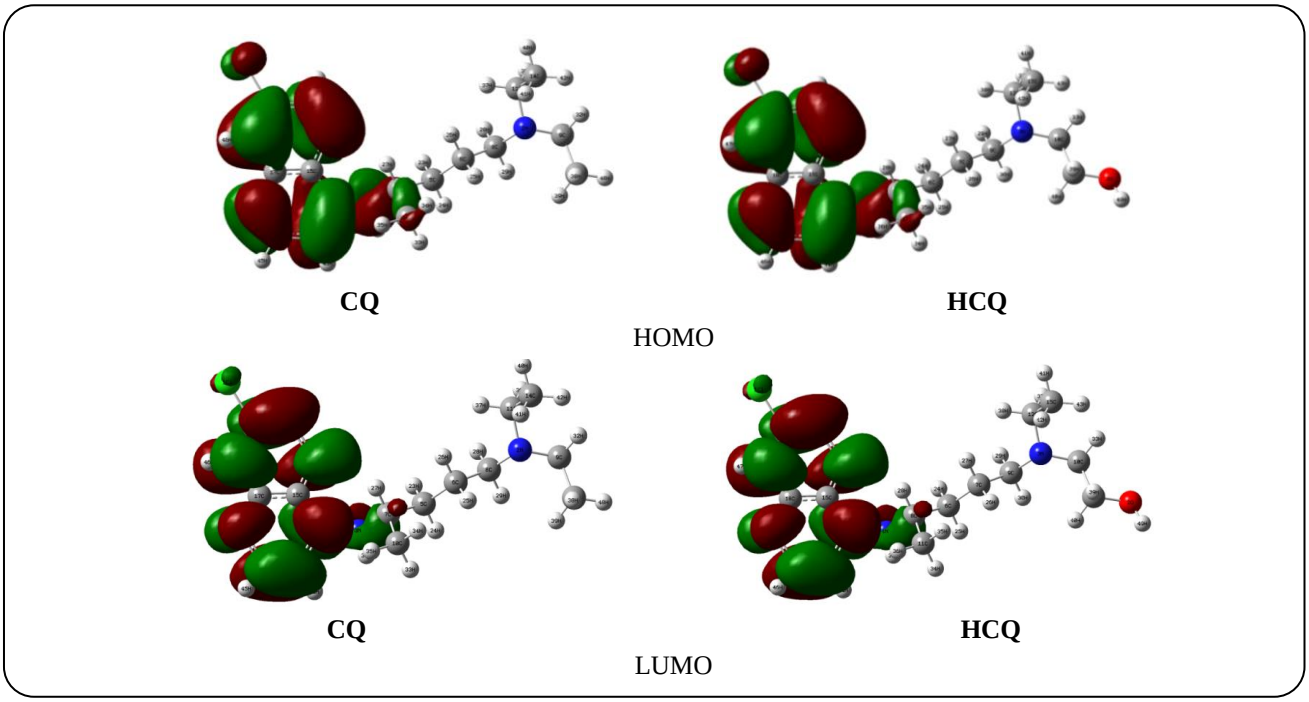

Fig. 4: HOMO and LUMO frontier orbitals of HCQ and CQ.

The calculated HOMO and LUMO orbitals for the HCQ and CQ molecules are illustrated in Fig. 4. The red and green solid surfaces characterize the molecular orbitals with fully opposite phases. The red color represents the positive phase of each molecule, while the green color indicates the negative phase. It can be seen from Fig. 4 that the HOMO and LUMO for both drug molecules are localized on the aromatic rings, chlorine atom (Cl), and the secondary amino group attached to the aromatic ring. Generally, these delocalized electrons work as binding regions to the receptor atoms. The calculated values of HOMO and LUMO energies presented in Table 2 indicate that the CQ has the highest values of E_{HOMO} and E_{LUMO} than those of HCQ, which indicates that the CQ releases electrons more than the HCQ. Also, we observe from the calculated values in Table 2 HCQ has the lower value of E_{LUMO}, which indicates its high capability to accept the electrons of the nucleophilic species. On the other hand, we observe that the obtained value of ΔE_{GAP} for the CQ is lower than those of HCQ, which reveals that the CQ is less stable and more reactive thane HCQ.

Molecular surface Electrostatic Potential (MEP)

The Molecular Electrostatic Potential (MEP) maps can be considered a useful way to locate the active sites assigned to the electrophilic and nucleophilic reactions. Generally, the MEP is related to the electronic density of a molecule and can indicate its electrostatic effect, partial charges, and chemical reactivity. Indeed, MEP maps furnish a visual technique to know the relative polarity of the molecule and to locate its negative and positive electrostatic potentials [32]. At any point in the space, the MEP is formed on the surface of the molecule by the total charge distribution is a practical guide to establishing the physical properties and molecular interactive manners. Also, the charge density, the form, the dimension, and the site of the chemical reactivity of a molecule can be characterized by the electron density isosurface mapped with the electrostatic potential surface. In general, the variation of the electrostatic potential values is figured by a gradient of colors. The shadows colored in red and yellow represent the negative electrostatic potential zones corresponding to the electrophilic reactions and to the attraction of the proton by the elevated electron density in the molecule, while the shadows colored in bleu characterize the positive electrostatic potential concerning the nucleophilic reactions and describe the repulsion of the proton by atomic nuclei in sections where low electrons density is present and the nuclear

Table 2: Calculated quantum chemical parameters of HCQ and CQ using DFT/B3LYP 6-31G (d,p) method.

Quantum chemical parameters	HCQ	CQ
E_{Tot} (eV)	– 37743.4676	– 35718.1028
E_{HOMO} (eV)	– 8.53893606	– 8.51009198
E_{LUMO} (eV)	2.16874826	2.19541543
ΔE_{GAP} (eV)	10.7076843	10.7055074
μ (Debye)	5.53130000	5.81920000
η (eV)	5.35384215	5.35275370
σ	0.18678175	0.18681973
χ (eV)	3.18509390	3.15733827
ω	0.94743391	0.93118286

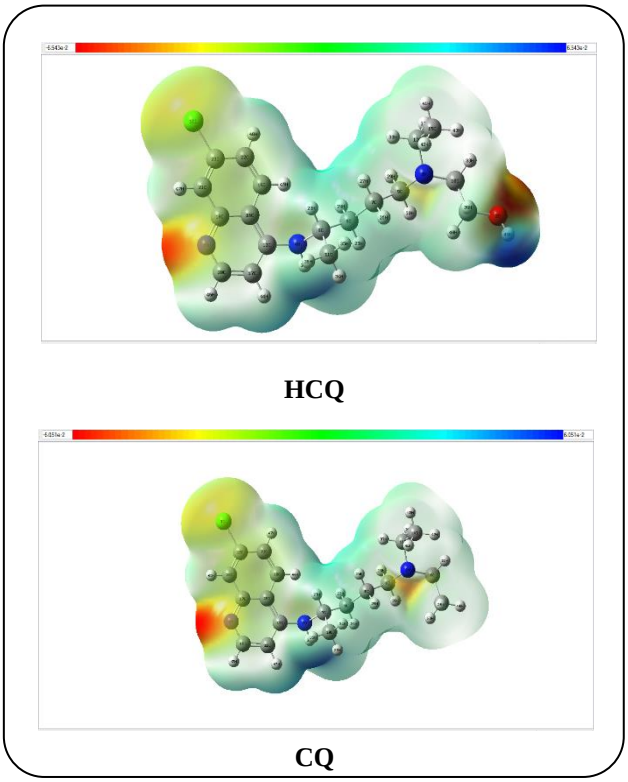

Fig. 5: Calculated 3D MEP maps of HCQ and CQ.

a charge is moderately covered. Further, the green shadows indicate the zone of nil potential and the increase of the potential follows the following sequence [33]:

red<orange<yellow<green <blue

Fig. 5 displays the obtained 3D MEP maps of HCQ and CQ using DFT calculations. The interpretation of the obtained 3D MEP maps indicates that the red and yellow zones are located on the Cl1, O2, N3, N4, and N5 atoms for the HCQ and the Cl1, N2, N3, and N4 atoms for the CQ, which indicates that all of these atoms are the probable sites of the electrophilic reactions. Also, the two aromatic rings of HCQ and CQ are considered negative zones. On the other hand, the blue and green zones have been observed around the carbon and hydrogen atoms, which reveal the positive regions responsible for the nucleophilic reactions, these regions reveal the presence of weak interactions.

The forms of the electrostatic potential are located near the polar groups in the HCQ and CQ molecules. In the studied molecules, the charge density distribution and the stereo structure affect the nitrogen of the amino group and the oxygen of the hydroxyl group. Also, the nitrogen site shows the region of most negative electrostatic potential and high activity of the imine group (C=N). On the other hand, the region near the polar chlorine atom show region of mildly negative. In addition, the zones of zero potential contain the hydrogen atoms of hydroxyl group and hydrogen atoms of the secondary amine and this indicates a high possibility for an electronegative substitution reaction.

Mulliken atomic charges

Generally, the analysis of Mulliken charges is provided to estimate the partial atomic charges of a molecule. Also, the Mulliken charge of atoms in drug molecules can be considered an adsorption center. From Table 3, which regroups the calculated atomic Mulliken charges of HCQ and CQ, we notice that the negative charges are accumulated on the nitrogen and oxygen atoms as a result of molecular relaxation. On the other hand, the positive charges are located on the hydrogen atoms at different values. Also, we note that the O2, the N3, the N4, and N5 atoms of HCQ and the N2, the N3, and N4 atoms of CQ have the most negative charges, which are maybe the active centers of fixation (adsorption) [34]. So, these heteroatoms (O and N) can participate in their electron pairs with an acceptor molecule. In addition, the C13 and C12 atoms of HCQ and CQ respectively have the most positive charges, which propose that the charge is widely delocalized in the entire molecule.

Table 3: Calculated Mullikan atomic charges of HCQ and CQ.

HCQ				CQ			
Atom	Mulliken Charge	Atom	Mulliken Charge	Atom	Mulliken Charge	Atom	Mulliken Charge
Cl1	0.0995720	H31	0.3249630	Cl1	0.0988180	H31	0.1803020
O2	-0.6905560	H32	0.2062490	N2	-0.6880950	H32	0.2153120
N3	-0.7139730	H33	0.2293980	N3	-0.8412200	H33	0.1909090
N4	-0.8409460	H36	0.2205990	N4	-0.7495030	H36	0.1816570
N5	-0.7491740	H37	0.1858220	C5	-0.3935110	H37	0.2105400
C6	-0.3938010	H38	0.2104590	C6	-0.4241210	H38	0.2151710
C7	-0.4246360	H39	0.1942360	C7	-0.0752540	H39	0.1960010
C8	-0.0747750	H40	0.1800440	C8	-0.1524980	H40	0.1913190
C9	-0.1471130	H41	0.1931030	C9	-0.1844990	H41	0.2142260
C10	-0.1905050	H42	0.2111540	C10	-0.5796180	H42	0.1995520
C11	-0.5797190	H43	0.2030050	C11	-0.1843690	H43	0.2402670
C12	-0.1774030	H44	0.2402240	C12	0.4181060	H44	0.2818230
C13	0.4174440	H45	0.2815080	C13	-0.5822650	H45	0.2573170
C14	-0.0653070	H46	0.2575170	C14	-0.5825260	H46	0.2973550
C15	-0.5851490	H47	0.2975590	C15	-0.1139830	H47	0.2741240
C16	-0.1138540	H48	0.2744090	C16	-0.3572020	H48	0.1910490
C17	-0.3570730	H49	0.3765310	C17	0.3095460		
C18	0.3095010			C18	-0.1954280		
C19	-0.1955710			C19	0.1546910		
C20	0.1546950			C20	-0.1455420		
C21	-0.1453870			C21	-0.1931390		
C22	-0.1929070			C22	-0.3226230		
C23	-0.3229270			H23	0.2236730		
H24	0.2251240			H24	0.1974510		
H25	0.1977270			H25	0.2268020		
H26	0.2221160			H26	0.2066530		
H27	0.2082430			H27	0.2426000		
H28	0.2429770			H28	0.1804580		
H29	0.1845660			H29	0.2109580		
H30	0.2085530			H30	0.3248170		

Dipole moment

The chemical reactivity of a molecule can be evaluated by measuring its dipole moment (μ). Generally, this parameter indicates the polarity of a molecule which is related to the distribution of the fractional electric charge in this molecule [35]. Also, the importance of this parameter lies in the reaction mechanism and indicates the capability of a molecule to react with another molecular species. The obtained values of μ for the studied drugs (Table 2) indicate that the HCQ and CQ present a high

ability to react and interact with the surrounding medium. Furthermore, we observe that CQ has an elevated value of μ than HCQ which indicates its high reactivity.

Global reactivity descriptors

In quantum chemical calculations, the obtained values of HOMO and LUMO energies are utilized to calculate the global reactivity descriptors such as hardness (η), local softness (σ), electronegativity (χ), and electrophilicity (ω). Generally, these quantum parameters are considered a link between global chemical reactivity and the stability of the molecular structures [36].

Hardness and local softness are considered important global reactivity descriptors that can be employed to evaluate the stability and chemical reactivity of a molecule. Generally, the hardness measures the resistance of molecules towards the polarization or deformation of their electron clouds. Also, the hard molecule is characterized by a large ΔE_{GAP}, while the soft molecule is described by a small ΔE_{GAP}. Table 2 shows that HCQ presents a high value of η and the low value of σ, which indicates that HCQ is more stable and less reactive than CQ.

The calculated values of electronegativity presented in Table 2 show that the HCQ has the highest electronegativity, which indicates that HCQ is the lowest electron donor. Furthermore, the electrophilicity of a molecule measures its ability to receive electrons. Also, the high value of ω characterizes a good electrophile, while the low value of ω indicates a good nucleophile [37]. Generally, the organic molecules can be classified according to their electrophilicity into three classes: marginal electrophiles with $\omega <$ 0.8 eV, moderate electrophiles with 0.8 $< \omega <$ 1.5 eV and strong electrophiles with $\omega >$ 1.5eV [38]. From Table 2 we observe that the investigated molecules are moderate electrophiles with 0.8 $< \omega <$ 1.5 eV. On the other hand, the obtained value of ω for HCQ is higher than it's for CQ, which indicates that the HCQ is the powerful electrophile and electron acceptor.

CONCLUSIONS

A quantum chemical study of Hydroxychloroquine (HCQ) and Chloroquine (CQ) drugs used as a treatment of COVID-19 has been performed using DFT method at B3LYP/6-31G (d.p) basis set. Also, the optimized molecular structures, the vibrational spectra, and the quantum chemical parameters have been determined for the studied drugs. In this context, we present below the main obtained conclusions. Firstly, the HCQ molecule is more stable than CQ. The IR spectra were calculated and the vibrational modes have been completely assigned. The obtained values of E_{HOMO} and E_{LUMO} indicate that the CQ donates electrons more than the HCQ. Also, the calculated values of ΔE_{GAP} reveal that the CQ is less stable and more reactive thane HCQ. The MEP maps results indicate that the probable sites of the electrophilic reactions are located on the chlorine, oxygen, and nitrogen atoms. The Mulliken charges analysis shows that the oxygen and nitrogen atoms may be the active centers of adsorption. Finally, the calculated global reactivity descriptors show that the HCQ is more stable, a powerful electrophile, less reactive, and an electron acceptor.

Acknowledgments

This research was supported by the General Directorate for Scientific Research and Technological Development (DGRSDT), Algerian Ministry of Scientific Research, Laboratory of Electrochemistry of Molecular Materials and Complex (LEMMC). University of Ferhat ABBAS Setif-1.

Received : May 16, 2020 ; Accepted : Sep. 22, 2020

REFERENCES

[1] Lai C.C., Shih T.P., Ko W.C., Tang H.J., Hsueh P.R., Severe Acute Respiratory Syndrome Coronavirus 2 (SARS-CoV-2) and Coronavirus Disease-2019 (COVID-19): The Epidemic and the Challenges, *Int J. Antimicrob Agents*, **55(3)**: 105924 (2020).

[2] Wang L., Wang Y., Ye D., Liu Q., Review of the 2019 Novel Coronavirus (SARS-CoV-2) Based on Current Evidence, *Int. J. Antimicrob Agents*, **55(6)**: 105948 (2020).

[3] WHO Director-General's opening remarks at the media briefing on COVID-19–11 March 2020. [https://www.who.int/dg/speeches/detail/who-director-general-s-opening-remarks-I-media-briefing-on-covid-19---11-march-2020]

[4] Gobato R., Mitra A., The Inside Story of Coronavirus Pandemic, *Parana Journal of Science and Education (PJSE)*, **6(3)**:9 3-100 (2020).

[5] Klaus N., Influence of Chlorine Substituents on Biological Activity of Chemicals: A Review, *Pest Manag. Sci.*, **56(1)**: 3–21 (2000).

[6] Henschler O., Toxikologie Chlororganischer Verbindungen, *Angew. Chemie.*, **107(8)**: 1017-1017 (1995).

[7] Hileman B., Concerns Broaden over Chlorine and Chlorinated Hydrocarbons, *Chem. Eng. News.*, **19(1)**: 11–20 (1993).

[8] Henschler D., Toxizität Chlororganischer Verbindungen: Einfluß der Einführung von Chlor in Organische Moleküle, *Angew. Chem.*, **106(19)**: 1997-2012 (1994).

[9] Wang M., Cao R., Zhang L., Yang X., Liu J., Xu M., Shi Z., Hu Z., Zhong W., Xiao G., Remdesivir and Chloroquine Effectively Inhibit the Recently Emerged Novel Coronavirus (2019-nCoV) *in Vitro*, *Cell Res*, **30(3)**: 269-271 (2020).

[10] Gao J., Tian Z., Yang X., Breakthrough: Chloroquine Phosphate Has Shown Apparent Efficacy in Treatment of COVID-19 Associated Pneumonia in Clinical Studies, *Biosci Trends*, **14(1)**:72-73 (2020).

[11] Chinese Clinical Trial Registry. http://www.chictr.org.cn/

[12] Gautret P., Lagier J.C., Parola P., Hoang V.T., Meddeb L., Mailhe M., Doudier B., Courjon J., Giordanengo V., Vieira V.E., Dupont H.T., Honoré S., Colson P., Chabrière E., La Scola B., Rolain J.M., Brouqui P., Raoult D., Hydroxychloroquine and Azithromycin as a Treatment of COVID-19: Results of an Open-Label Non-Randomized Clinical Trial, *International Journal of Antimicrobial Agents*, **56(1)**: 105949 (2020).

[13] Zhou D., Dai S.M., Tong Q., COVID-19: A Recommendation to Examine the Effect of Hydroxychloroquine in Preventing Infection and Progression, *J Antimicrob Chemother*, **75(7)**: 1667-1670 (2020).

[14] Schrezenmeier E., DörnerT., Mechanisms of Action of Hydroxychloroquine and Chloroquine: Implications for Rheumatology, *Nat Rev Rheumatol*, **16(3)**: 155–166 (2020).

[15] Oftadeh M., Madadi Mahani N., Hamadanian M., Density Functional Theory Study of the Local Molecular Properties of Acetamide Derivatives as Anti-HIV Drugs, *Res Pharm Sci*, **8(4)**: 285–297 (2013).

[16] Behzadi H., Roonasi P., Taghipour K.A., Van der Spoel D., Manzetti S., Relationship between Electronic Properties and Drug Activity of Seven Quinoxaline Compounds: A DFT Study, *J. Mol. Struct*, **1091(13)**: 196-202 (2015).

[17] Tariq A., Nazir S., Arshad A.W., Nawaz F., Ayub K., Iqbal J., DFT Study of the Therapeutic Potential of Phosphorene as a New Drug-Delivery System to Treat Cancer, *RSC Adv*, **9(42)**: 24325-24332 (2019).

[18] Hellal A., Chafaa S., Chafai N., Touafri L., Synthesis, Antibacterial Screening and DFT Studies of Series of A-Amino-Phosphonates Derivatives from Aminophénols, *J. Mol. Struct*, **1134(8)**: 217–225 (2017).

[19] Mehri M., Chafai N., Ouksel L., Benbouguerra K., Hellal A., Chafaa S., Synthesis, electrochemical and classical evaluation of the antioxidant activity of Three α-aminophosphonic Aacids: Experimental and theoretical investigation, *Journal J. Mol. Struct*, 1171(21):179 □ 189 (2018).

[20] Hellal A., Chafaa S., Chafai N., Synthesis, Antibacterial and Antifungal Screening of Three New of Alpha-aminophosphonic Acids, *International Journal of Scientific & Engineering Research*, 6(8):1622 □ 1627 (2015).

[21] Pandey A.K., Mishra V.N., Singh V., Biological, Electronic, NLO, NBO, TDDFT and Vibrational Analysis of 1-benzyl-4-formyl-1H-pyrrole-3-Carboxamide, *Iran. J. Chem. Chem. Eng.(IJCCE)*, 39(1):233-242 (2020).

[22] Frisch M.J., Trucks G.W., Schlegel H.B., Scuseria G.E., Robb M.A., Cheeseman J.R., Scalmani G., Barone V., Mennucci B., Petersson G.A., Nakatsuji H., Caricato M., Li X., Hratchian H.P., Izmaylov A.F., Bloino J., Zheng G., Sonnenberg J..L., Hada M., Ehara M. , Toyota K, Fukuda R., Hasegawa J., Ishida M., Nakajima T., Honda Y., Kitao O., Nakai H., Vreven T., Montgomery Jr. J.A., Peralta J.E., Ogliaro F., Bearpark M., Heyd J.J., Brothers E., Kudin K.N., Staroverov V.N., Kobayashi R., Normand J., Raghavachari K., Rendell A., Burant J.C., Iyengar S.S., Tomasi J., Cossi M., Rega N., Millam J.M., Klene M., Knox J.E., Cross J.B., Bakken V., Adamo C., Jaramillo J., Gomperts R., Stratmann R.E., Yazyev O., Austin A.J., Cammi R., Pomelli C., Ochterski J.W., Martin R.L., Morokuma K., Zakrzewski V.G., Voth G.A., Salvador PDannenberg., J.J., Dapprich S., Daniels A.D., Farkas O., Foresman J.B., Ortiz J.V., Cioslowski J., Fox D.J., "Gaussian 09, Revision A.02, Gaussian", Inc., Wallingford, CT, (2009).

[23] Chafai N., Chafaa S., Benbouguerra K., Hellal A., Mehri M., Synthesis, Spectral Analysis, Anti-Corrosive Activity and Theoretical Study of an Aromatic Hydrazone Derivative, *J. Mol. Struct*, **1181(7)**: 83-92 (2019).

[24] Benbouguerra K., Chafaa S., Chafai N., Mehri M., Moumeni O., Hellal A., Synthesis, Spectroscopic Characterization and a Comparative Study of the Corrosion Inhibitive Efficiency of an A-Aminophosphonate and Schiff Base Derivatives: Experimental and Theoretical Investigations, *J. Mol. Struct*, **1157(7)**: 165–176 (2018).

[25] Chafai N., Chafaa S., Benbouguerra K., Daoud D., Hellal A., Mehri M., Synthesis, Characterization and the Inhibition Activity of a New α-aminophosphonic Derivative on the Corrosion of XC48 Carbon Steel in 0.5 M H_2SO_4: Experimental and Theoretical Studies, *J. Taiwan Inst. Chem. Eng*, **70(1)**:331–344 (2017).

[26] Djenane M., Chafaa S., Chafai N., Kerkour R., Hellal A., Synthesis, Spectral Properties and Corrosion Inhibition Efficiency of New Ethylhydrogen [(methoxyphenyl) (36 ethyl amino)methyl] phosphonate Derivatives: Experimental and Theoretical Investigation, *J. Mol. Struct*, **1175(1):**398-413 (2018).

[27] Hong L.X., Ru L.X., Zhou Z.X., Calculation of Vibrational Spectroscopic and NMR Parameters of 2-Dicyanovinyl-5-(4-N,N-dimethylaminophenyl) Thiophene by ab Initio HF and Density Functional Methods, *Comput. Theor.Chem*, **969(1-3):** 27-34 (2011).

[28] Elmi S., Foroughi M.M., Dehdab M., Shahidi-Zandi M., Computational Evaluation of Corrosion Inhibition of Four Quinoline Derivatives on Carbon Steel in Aqueous Phase**,** *Iran. J. Chem. Chem. Eng (IJCCE).*, **38(1)**: 185-200 (2019).

[29] Khaled K.F., Studies of Iron Corrosion Inhibition Using Chemical, Electrochemical and Computer Simulation Techniques, *Electrochim Acta*, **55(22)**: 6523-6532 (2010).

[30] Lgaz H., Bhat K.S., Salghi R., Shubhalaxmi, Jodeh S., Algarra M., Hammouti B., Ali I.H., Essamri A., Insights into Corrosion Inhibition Behavior of Three Chalcone Derivatives for Mild Steel in Hydrochloric Acid Solution, *J. Mol. Liq*., **238(13)**: 71–83 (2017).

[31] Fliszar S., "Charge Distributions and Chemical Effects", Springer, New York (1983).

[32] Silverstein R.M., Webster F.X., "Spectroscopic Identification of Organic Compounds", John Wiley & Sons, Inc., New York (1998).

[33] Yesilkaynak T., Binzet G., Emen F.M., Florke U., Kulcu N., Arslan H., Theoretical and Experimental Studies on N-(6-methylpyridin-2-yl-carbamothioyl) biphenyl-4-carboxamide, *Eur. J. Chem*, **1(1)**: 1-5 (2010).

[34] Moumeni O., Chafaa S., Kerkour R., Benbouguerra K., Chafai N., Synthesis, Structural and Anticorrosion Properties of Diethyl(phenylamino)methyl) Phosphonate Derivatives: Experimental and Theoretical Study, *J. Mol. Struct*, **1206(8)**: 127693 (2020).

[35] Issa R.M., Awad M.K., Atlam F.M., Quantum Chemical Studies on the Inhibition of Corrosion of Copper Surface by Substituted Uracils, *Appl. Surf. Sci*, **255(5)**:2433–2441 (2008).

[36] Vijayaraj R., Subramanian V., Chattaraj P.K., Comparison of Global Reactivity Descriptors Calculated Using Various Density Functionals: A QSAR Perspective, *Journal of Chemical Theory and Computation*, **5(10)**: 2744- 2753 (2009).

[37] Hellal A., Chafaa S., Chafai N., Synthesis, Characterization and Computational Studies of Three α-amino-phosphonic Acids Derivatives from Meta, Ortho and Para Aminophenol, *J. Mol. Struct*, **1103(1)**: 110–124 (2016).

[38] Domingo L.R., Aurell M.J., Pérez P., Contreras R., Quantitative Characterization of the Global Electrophilicity Power of Common Diene/Dienophile Pairs in Diels-Alder Reactions, *Tetrahedron*, **58(22)**: 4417–4423 (2002).